**Proceedings of the ASME 2010 3rd Joint US-European Fluids Engineering Summer Meeting and 8th International Conference on Nanochannels, Microchannels, and Minichannels**
**FEDSM-ICNMM2010**
**August 1-5, 2010, Montreal, Canada**

# FEDSM-ICNMM2010-31073

## SIMULATION OF DRIPPING FLOW USING DISSIPATIVE PARTICLE DYNAMICS

**Sorush Khajepor** **Meysam Joulaian**

**Ahmadreza Pishevar** **Yaser Afshar**

Department of Mechanical Engineering, Isfahan University of Technology
Isfahan, 84156-83111, Iran

### ABSTRACT

Dissipative Particle Dynamics (DPD) is a mesoscopic simulation approach used in wide range of applications and length scales. In this paper, a DPD simulation is carried out to study dripping flow from a nozzle. The results of this study are used to answer this question that whether DPD is capable of simulating the free surface fluid on all different scales.

A novel wall boundary condition is developed for the nozzle surface that controls its penetrability, near wall fluid density oscillations and the fluid slip close to the wall. We also utilize a new method to capture the real-time instantaneous geometry of the drop. The obtained results are in good agreement with the macroscopic experiment except near the breakup time, when the fluid thread that connects the primitive drop to the nozzle, becomes tenuous. At this point, the DPD simulation can be justified by thermal length of DPD fluid and the finest accuracy of the simulation that is the radius of a particle. We finally conclude that in spite of the fact that DPD can be used potentially for simulating flow on different scales, it is restricted to the nanoscale problems, due to the surface thermal fluctuations.

### INTRODUCTION

When a fluid is continuously delivered from a nozzle into an immiscible and inert medium, two modes of flow regime can be formed: dripping and jetting. Occurrence of each mode depends on the quantity of the governing dimensionless numbers e.g. Ohnesorge number, Bond number and Weber number [1]. Dripping mode is an active area of interest and it has applications in a number of technological processes including inkjet printing [2], spraying[3], separation processes [4]. Dripping flow has also been studied by many researchers, experimentally [5] or numerically [6] in macroscale problems. When the length and time scale is reduced to the mesoscale levels, atomistic fluctuation play a key role in the flow pattern in the dripping mode and another dimensionless number, thermal length, becomes important. Thermal fluctuations cannot be captured by experiment and they can no longer be justified with the continuum perturbation theory [7]. DPD is an eligible method to study this category of problems because it is able to highlight the importance of thermal fluctuations.

DPD is applied to simulate problems in different scales. Kumar et al. [8] have simulated fluid flow in a microchannel. Füchslin et al. [9] have shown that the single phase DPD is not only a mesoscale method but also a free scale method. Clark et al. [10] simulated multi-component breakup of a micro drop in shear field. Tiwari and Abraham [11] simulated breakup of a nanojet of a two-phase fluids. The motivation of the present study is to answer this question that whether DPD is a free scale method for simulating two-phase flows or free surface flows. Hence, a DPD simulation of dripping is planned to achieve the same Ohnesorge number, Bond number and Weber number of an available macroscopic experiment.

Adjusting DPD parameters to simulate a specific physical problem is still an open area of interest, due to the fluid properties and kinematic variables in DPD simulation which

 

are in reduced units. To reach this aim, we present a different approach by introducing the concept of dimensionless numbers. By duplicating these numbers to the real physics for a DPD fluid, we can explicitly establish a relation between the DPD simulation fluid parameters to those of a mixture of 85% glycerol by weight in water dripping from a 1600 $\mu m$ nozzle.

In our simulation, the nozzle surface is constructed with the frozen particles and its impenetrability, proper surface wettability, ability to eliminate density oscillation near the wall and no-slip boundary condition are attained by manipulating the coefficient of conservative forces between the wall particles and the fluid particles. In order to capture the instantaneous geometry of the drop on a Cartesian grid, we assumed that DPD particles must have a volume mass rather than a point mass that carry data through the domain.

At last we show that our simulation can be corresponded to the physics of a dripping flow from a nanoscale nozzle and not a macroscopic one.

## METHODOLOGY

A. Dissipative Particle Dynamics

In DPD simulation each particle represents a cluster of atoms or molecules called DPD particle. Movement of DPD particles is governed by the Newton second's law:

$$\frac{\partial \vec{r}_i}{\partial t} = \vec{v}_i \ , \ m_i \frac{\partial \vec{v}_i}{\partial t} = \vec{f}_i \tag{1}$$

where $\vec{r}_i$ and $\vec{v}_i$ are the respective position and velocity of ith DPD particles. The total force acting on these particles $\vec{f}_i$ is given by [12]:

$$\vec{f}_i = \sum_j \vec{F}_{ij}^{C} + \vec{F}_{ij}^{D} + \vec{F}_{ij}^{R} \tag{2}$$

where $\vec{F}_{ij}^{C}$ , $\vec{F}_{ij}^{D}$ and $\vec{F}_{ij}^{R}$ are called conservative, dissipative and random force, respectively and defined as:

$$\vec{F}_{ij}^{C} = a_{ij}\,\omega^{C}(r_{ij}, r_c)\hat{e}_{ij} \tag{3}$$

$$\vec{F}_{ij}^{D} = -\gamma_{ij}\,\omega^{D}(r_{ij}, r_c)\left(\hat{e}_{ij} \cdot \vec{v}_{ij}\right)\hat{e}_{ij} \tag{4}$$

$$\vec{F}_{ij}^{R} = \sigma_{ij}\,\omega^{R}(r_{ij}, r_c)\,\theta_{ij}\,\delta t^{-1/2}\hat{e}_{ij} \tag{5}$$

Here $\vec{r}_{ij} = \vec{r}_i - \vec{r}_j$, $\hat{e}_{ij} = \vec{r}_{ij} \big/ \left|\vec{r}_{ij}\right|$, $\vec{v}_{ij} = \vec{v}_i - \vec{v}_j$ and $\theta_{ij}$ is a random number drawn from a Gaussian statistics and has zero mean and unit variance. $a_{ij}$ , $\gamma_{ij}$ and $\sigma_{ij}$ determine the strength of the conservative, dissipative and random forces, respectively. These forces are pair-wise and effective in a certain distance, called cutoff radius $r_c$ . The weight functions are continuous functions of the distance, given by:

$$\omega^{C} = \omega^{R} = \sqrt{\omega^{D}} = \max\left[\left(1 - r_{ij}/r_c\right), 0\right] \tag{6}$$

Español and Warren [13] showed through the fluctuation-dissipation theorem that the below relation must be satisfied for the thermal equilibrium:

$$\sigma^2 = 2\gamma k_B T \tag{7}$$

where $T$ is the system temperature and $k_B$ is the Boltzmann constant.

B. Free surface DPD fluid

In DPD simulation, free surface fluid is formed by changing conservative forces. If the repulsion conservative forces of DPD are substituted with long range attraction and short range repulsion conservative forces, DPD will be able to construct an interface with vacuum [14]:

$$\begin{aligned} \vec{F}_{ij}^{C} &= A\ \omega^{C}(r_{ij}, r_c)\hat{e}_{ij} && A < 0 \\ &+ B\left(\rho_i + \rho_j\right)\omega^{C}(r_{ij}, 0.75 r_c)\hat{e}_{ij}\ , && B > 0 \end{aligned} \tag{8}$$

where the first term is the attraction and the second term is the repulsion part of conservative forces. Here $\rho_i$ is the instantaneous local density and is defined as:

$$\rho_i = \sum_{j \neq i} w_p(r_{ij}, r_c) \tag{9}$$

where sum runs over all neighboring particles and $w_p$ is:

$$w_p(r_{ij}, r_c) = \max\left[15/(2\pi r_c^3)(1 - r/r_c)^2, 0\right]. \tag{10}$$

## WALL BOUNDARY CONDITION

Implementing a proper wall boundary condition is necessary for simulating fluid flow inside the nozzle. The nozzle wall must produce a favorite velocity profile and its tip must control its wettability. In DPD, wall boundary condition is satisfied by using frozen particles that do not contribute in the integration of equation of motion. Soft inter-particle forces let particles penetration into the wall. To overcome this problem in the simulation of fluid flow near the wall, we utilized conservative forces instead of interaction rules between fluid and wall particles .e.g. bounce back [15]. In fact conservative forces between fluid and wall particles control wall penetrability, fluid density oscillations and fluid slip close to the wall. In the case of stationary fluid, they are employed to mimic correct contact angle at the solid boundaries.

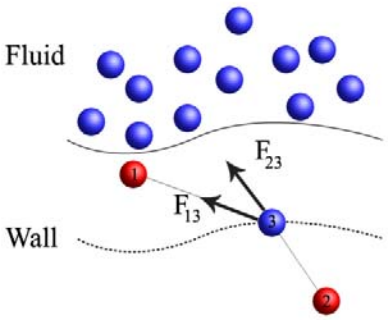


**Figure 1: The penetrated particle is subjected to forces that returns it into the fluid area**

When a particle penetrates into the wall, the conservative forces between that particle and the wall is adjusted as follows:

$$\vec{F}_{ij} = 2C(\rho_i + \rho_j)\omega^C(r_{ij}, 0.75r_c)\hat{e}_{ij} \qquad (11)$$

where $\rho$ is the local density approximated by Eq. (9) and C is a coefficient that the position of a penetrated particle determines its sign. We imagine a surface parallel to the wall-fluid interface which encompasses the penetrated particle; wall particles that are located above this surface attract penetrated particle with negative conservative forces and wall particles that are below it, repel the penetrated particle with positive conservative forces (see Figure 1). In fact "force back" obliges the penetrated particle to restore in the fluid area. Therefore wall penetrability is determined by magnitude of C. An initial guess for C would be the coefficient of fluid repulsion force, Eq. (8).

We can control fluid density oscillation and fluid slip close to the wall by adjusting the coefficient of conservative forces between wall and fluid ($A_{12}$ and $B_{12}$). Because of the short range nature of the repulsion force, increasing $B_{12}$ leads to a decrease in the fluid density and an increase in fluid slip very close to the wall. On the other hand decreasing $A_{12}$ diminishes long range effect of the wall on the fluid.

The proposed boundary conditions are validated by simulating a free surface flow on an inclined plane. A column of fluid with thickness of $8\,r_c$ is place on a wall of $2\,r_c$ thickness. The imposed body force vector components are 0.03 DPD units on the flow direction (x direction) and 0.1 DPD units on the direction perpendicular to the wall-fluid interface (z direction). Simulation domain is periodic in x and y directions. The simulation parameters are the same as those in Table 1 except for $\gamma$ which is set to be 12.5. For these system parameters, the fluid viscosity measured by Lees Edward method [16] is $\mu = 6.66$. We investigate three scenarios for $A_{12}$ and $B_{12}$ coefficients. The system is run for more than $10^4$ time steps to ensure us that flow is steady state. The density and velocity

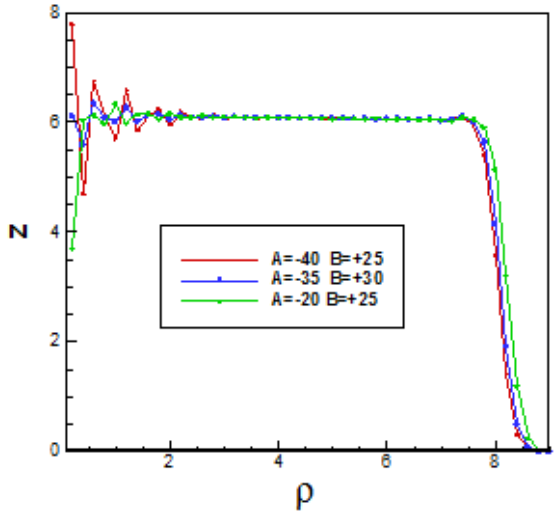


**Figure 2: Density profile of flow on the inclined plane**

profile in each case are obtained by averaging over $10^5$ time steps and shown in Figure 2 and Figure 3.

When $A_{12} = -40$, $B_{12} = +25$ are the same as fluid conservative forces, force back is active and $C = +25$: only 2 particles per 10 unit of area are penetrated into the wall but when force back parameter is switched off, 1 particle per unit of area is penetrated. Therefore force back could make the wall almost impenetrable. Figure 2 shows that some fluid density oscillation can be seen close to the wall. These oscillations may be considered desirable and physical but near to the continuum scale they are unacceptable. In spite of density oscillation, velocity profile is in good agreement with continuum results and the no-slip boundary condition is achieved (see Figure 3 ).

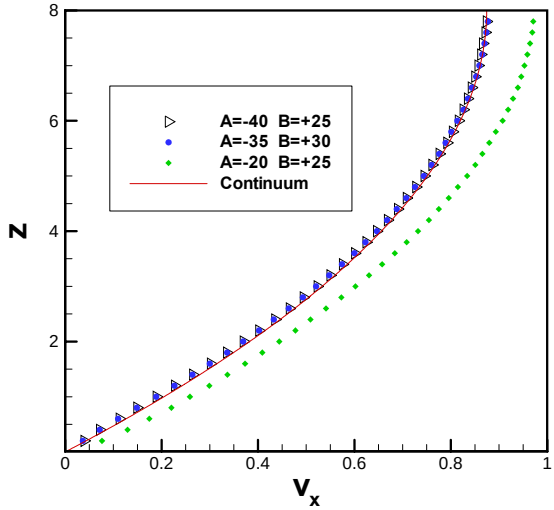


**Figure 3: velocity profile of flow on the inclined plane**

**Table 1 Parameters of DPD simulation**

| | | |
|---|---|---|
| Temperature | $k_B T$ | 1 |
| Particle mass | $m$ | 1 |
| Cutoff radius | $r_c$ | 1 |
| Fluid attraction amplitude | $A_{11}$ | -40 |
| Fluid repulsion amplitude | $B_{11}$ | +25 |
| Dissipative force amplitude | $\gamma$ | 12.92 |
| Time step | $\delta t$ | 0.02 |

For the second scenario, we increase repulsion conservative force to $B_{12} = +30$ to reduce the first peak of density oscillations and decrease the attraction to $A_{12} = -35$ to reduce the long range effect of the wall on the fluid particles. Thus, as illustrated in Figure 2 a nearly flat density profile is achieved while the velocity profile is unaltered and matched with the continuum velocity profile.

When repulsion force is fixed at $B_{12} = +25$ and the strength of attraction force is reduced to $A_{12} = -20$, the slip boundary condition is dominant and particles density deplete near the wall (see Figure 2 ), similar to the result when the repulsion force is increased in the ordinary DPD [15]. Hence in the third situation the velocity profile deviates from the continuum result (see Figure 3).

## SIMULATIONS

Consider a nozzle of radius $R$ that a fluid which can form a free surface with viscosity $\mu$, density $\rho$ and surface tension $\Gamma$ emerges from its tip by imposing a low flow rate at the inlet. In this case, discrete drops are formed from the nozzle in gravitational acceleration g. We also intend to simulate the dripping of a mixture of 85% glycerol by weight in water from a nozzle of radius 1600 $\mu m$ . Table Table 22 lists the properties and the values of the dimensionless numbers corresponding to the assumed liquid and the nozzle dimension[5]. In follow, we describe how the DPD system parameters and the boundary conditions are set for such an experiment.

A. How to map the physical parameters into the DPD system

An important part of the DPD simulation is to relate simulation parameters to the physical problem. Dimensionless numbers which reflect significant physical features of a problem can be used as a convenient way of establishing this relation. Dripping is governed by three dimensionless numbers [5]: Weber number $We = \rho u^2 R / \Gamma$ that measures the ratio of inertial force to the surface tension force, Ohnesorge number $Oh = \mu / \sqrt{\rho R \Gamma}$ that measures the ratio of viscous force to the surface tension force and the gravitational Bond number $G = \rho g R^2 / \Gamma$ that measures the ratio of gravitational force to the surface tension force. Therefore, these dimensionless numbers are used to calculate DPD parameters.

**Table 2 Properties of mixture of 85% glycerol and dimensionless numbers used in experiment and DPD simulation**

| Property | Physical system | DPD system |
|---|---|---|
| $\rho$ | $1.223\ g/cm^3$ | 6.06 |
| $\mu$ | $1.129\ g/cm\,s$ | $6.73 \pm 0.05$ |
| $\Gamma$ | $66.0\ g/s^2$ | $7.47 \pm 0.05$ |
| R | $1600\ \mu m$ | 10.15 |
| u | $2.07\ mm/s$ | 0.004 |
| g | $9.81\ m/s^2$ | 0.006 |
| We | 1.27e-4 | 1.27e-4 |
| Oh | 0.31 | 0.31 |
| G | 0.47 | 0.47 |

A common way to determine the coefficient of conservative force is to match the compressibility of the DPD system with the physical system [17]. However, if we suppose that the thermodynamic state is almost unaltered for the problem under investigation, the conservative forces can be employed to achieve the correct interfacial properties at the free surface. We select the coefficients of conservative forces between particles of fluid to be $A_{11} = -40$, $B_{11} = +25$ which results in a free surface fluid model with sharp interface and density equal to $\tilde{\rho} = 6.06$ [14]. When $r_c$ is equal to unit, because of computational costs, density number is kept around the order of unity as well. It is noted that temperature, mass and cutoff radius of DPD system are in reduced unit (i.e. $\tilde{k}_B \tilde{T} = \tilde{m} = \tilde{r}_c = 1$). For the selected conservative coefficients, the surface tension of DPD model is measured to be $\tilde{\Gamma} = 7.47 \pm 0.05$ as described in [14] (variables with hat illustrate DPD system variables, so the units of them are not mentioned).

In order to determine the radius of nozzle in DPD unit $l_\mu = \mu^2 / \rho\sigma$ can be an appropriate length scale for constructing the dimensionless numbers, because the fluid behavior near the pinch point in the macroscopic scales only depends on its intrinsic properties and pinching occurrs at $l_\mu$ scale [18]. Therefore, the cutoff radius is set to $r_c = l_\mu$. As a result, the viscosity of the DPD fluid is determined to be $\tilde{\mu} = 6.73$.

Viscosity of a DPD fluid can be changed by varying the coefficient of dissipative force without significantly affecting the other properties. The suitable coefficient that obliges the fluid to have a predefined viscosity can be obtained by performing several Lees-Edward shear simulations [16] and interpolating between the sample results; in this case, this coefficient is found to be $\gamma = 12.92$. Finally, the coefficient of the random force is calculated from the fluctuation-dissipation theory Eq.(7). The DPD simulation parameters are presented in Table 1.

By duplicating Oh number between the DPD and the physical system, nozzle radius in DPD system is achieved to be

$\tilde{R} = 10.15$. By duplicating the two other dimensionless numbers, G and We, the gravity and flow rate can be determined as $\tilde{g} = 0.006$ and $\tilde{u} = 0.004$ , respectively, in DPD system. The properties and kinematics variables of DPD fluid and their corresponding physical values are listed in Table 2.

B. Simulation of Dripping

The frozen nozzle particles are extracted from the homogeneous distribution of the particles achieved by performing an independent simulation of the free surface fluid in a periodic box. The inner radius of the nozzle is set to $\tilde{R}_i = 0.5\tilde{R}$ where R is the outer radius of the nozzle tip. The nozzle is composed of three types of frozen particles: tip (2), wall (3) and piston (4) (see Figure 4), so with the fluid (1) itself four types of particles exist in the simulation.

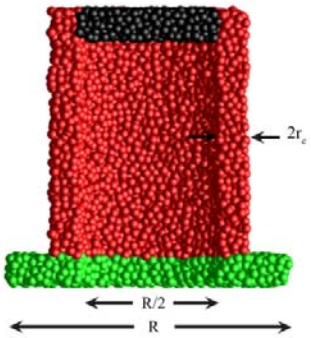


**Figure 4: Geometry of nozzle; black particles show piston, red particles are wall and green particles show tip of the nozzle**

In order the fluid particles to be able to wet the tip surface as in the experiment, the conservative forces between the tip nozzle particles and the fluid particles must be the same as in the fluid/fluid interactions (i.e. $A_{12} = A_{11}$ and $B_{12} = B_{11}$). We aim to simulate the nozzle flow in a millimeter scale so the density oscillations near the wall are not captured and no-slip boundary condition is dominated. Consequently, the conservative forces between the nozzle wall and the fluid are set to $A_{13} = -35$ and $B_{13} = +30$. Conservative coefficients for the piston/fluid particle interactions are the same as the nozzle wall/fluid interactions, except for their velocity which is set to $\tilde{u}$. During the simulation, in every specific time interval, some new fluid particles are introduced close to the piston to satisfy the inflow boundary condition. The production rate of these particles is constant and corresponds to the physical value. The height of nozzle is long enough, $\tilde{h} = 40$, to ensure us that the disturbance of the new generated particles is damped and a steady flow forms at the nozzle exit. The downward gravitational force, $\tilde{g}$, is applied to each fluid particle. By advancing in time, the exited particles wet the nozzle tip surface and gradually form a spherical drop, as seen in Figure 6.

C. Capture instantaneous drop geometry

The geometry of DPD drop must be analyzed within the simulation as part of the comparison with the experiment. A common approach to find the drop interface is to divide the simulation domain into a finite number of cells and then compute the corresponding cell fluid density by considering the number of particles which occupy that cell. This approach leads to an accurate result for stationary flow geometry where the averaging process can be performed over many time steps. In such a case, the longer averaging time interval results in a more accurate density profile. But this method is not applicable to the problems in which the flow geometry is changing during the simulation. In this case, when density is calculated in every time step, it is very likely to face some empty cells within the fluid region as a result of small cell size. Therefore, a different approach is adopted. In this approach, the DPD particles are assumed to have a volume mass rather than a point mass that carries data through the domain. Here the simulation box is covered by finite number of nodes and the effects of each particle volume are considered on the nearby nodes with a weight function. In contrast to the local density calculation [19], here there is no advantage for selecting a particular weight function because we are only interested in finding nodes which are close to the interface and the accuracy of the local density is not important.

The radius of a particle is computed from:

$$r_p = \frac{3}{4\pi}(N_m \, m_{mol} / \rho)^{1/3}$$

where $m_{mol}$ is the mass of each fluid molecule. The radius of a particle is calculated to be $5.373 \times 10^{-5}$ m and when converted to the DPD unit using Table 2 it becomes $\tilde{r}_p = 0.34$.

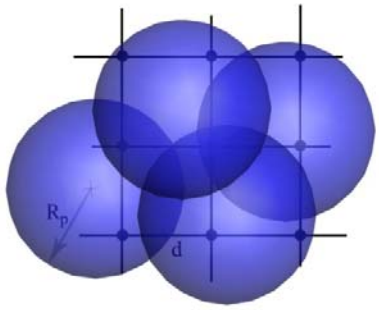


**Figure 5: the effects of each particle volume is considered on its neighbor nodes**

The method is accurate when the length scale is larger than the radius of a particle. Using this grid size, each particle can affect 8 nodes of the Cartesian grid (see Figure 5). This leads to a smoother drop profile and almost all of the interface nodes that form the drop geometry are recognized. This profile will be

utilized to calculate the real-time minimum radius of the drop and the length from its tip up to the nozzle outlet at the necking process.

## RESULTS AND DISCUSSION

Figure 6 shows few snapshots of the drop formation and the evolution of the thread that connects the falling drop to the remainder of the liquid in the nozzle during the necking and breakup process. The time difference is given in DPD units and is measured from the breakup time $t_b$ as a reference. As shown in the figure, as the drop size is increased in time, the shape of the drop is transformed to a pear shape and finally a neck is developed near the nozzle tip.

In all stages of the simulation some surface fluctuations are observed while in the experimental results the surface is obviously smooth [5]. On the other hand, we expect for the 85% glycerol mixture to develop a secondary neck in this scale. However, in the present simulation, the surface fluctuations prevent the formation of the secondary neck and instead cause an early break up in the primary thread.

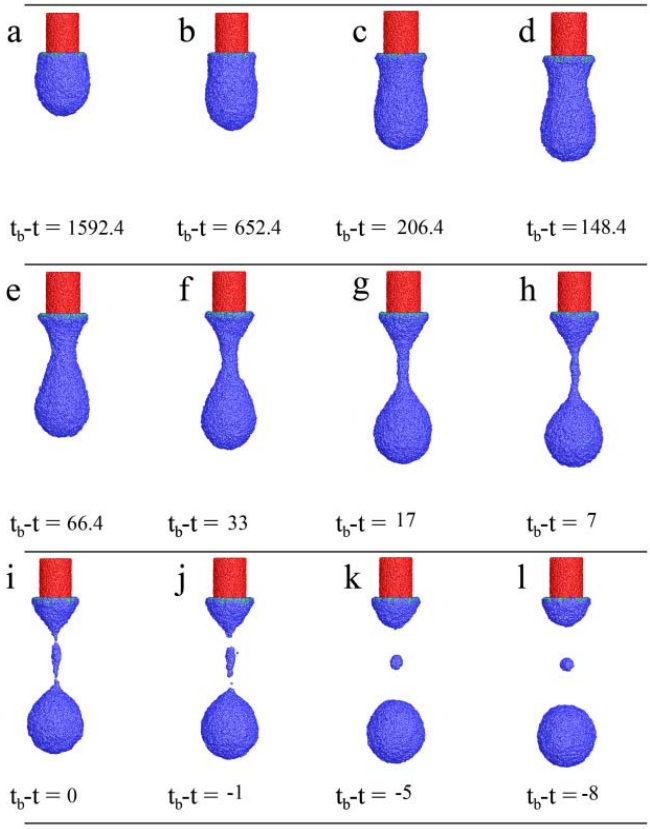


**Figure 6: snapshots of the Drop formation, its evolution in time and its beakup**

Moseler and landman [20] through a MD simulation have shown that this surface fluctuation can be observed in a system which size is in the order of the thermal length scale $l_T = \sqrt{k_B T / \Gamma}$. This length is about 1nm for the most liquids at the room temperature. Therefore, in this length scale the thermal fluctuations almost alters the characteristics of the breakup and speeds up the process by making the surface tension insignificant [7]. Thermal length in our simulation is $l_T = 0.37$.

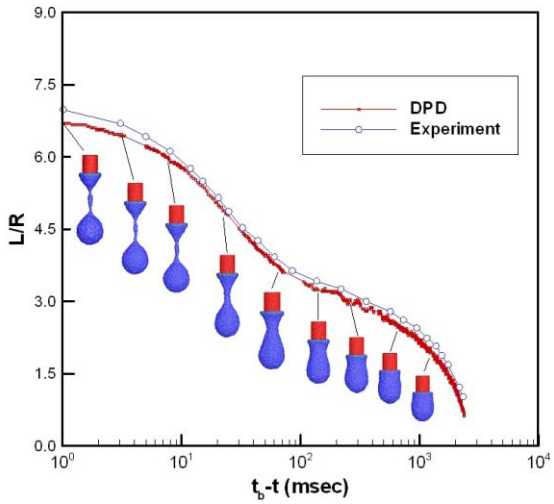


**Figure 7: evolution in time of the dimensionless length of the experimental [5] drop and the DPD drop according to their $t_b$**

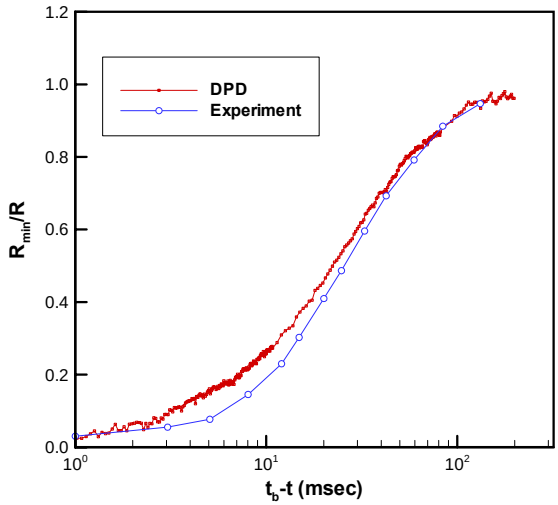


**Figure 8: evolution in time of the dimensionless minimum radius for the experimental [5] thread and the DPD thread according to their $t_b$**

As seen in Figure 6, when the radius of fluid approaches to $l_T$, a symmetric double-cone structure is formed at the location where primary thread begins to thin. Figure 7 shows a comparison between the experimental [5] and the DPD numerical results for the evolution of the thread dimensionless length in time with $t_b$ as the reference time. Figure 8 shows the thinning trend of the minimum radius for the experimental

thread [5] and the DPD thread according to their $t_b$. The time of both the experiment and the DPD simulation is given in milliseconds.
As seen in this figures, the DPD results follow the experiment up to the break up point. However, the surface fluctuation of DPD fluid is clearly seen in Figure 7 and Figure 8.

As spelled out earlier, the thermal noise speeds up the breakup, so the rupture of DPD simulation happens faster than the experiment i.e. $t_b$ of DPD is less than $t_b$ for the experiment ( $t_b^{DPD} < t_b^{\exp}$). Therefore, for the comparison sake, the time reference $t_b^{DPD}$ is shifted 2ms sooner.. This leads to a better agreement between the experimental and the DPD results for the evolution of dimensionless thread length as shown in Fig. 9. Moreover, the minimum radius of the thread achieves a better agreement with the experiment as the radius of the neck approaches $l_T$, as seen in Figure 10. In this situation the thread quickly thins and the breakup occurs.

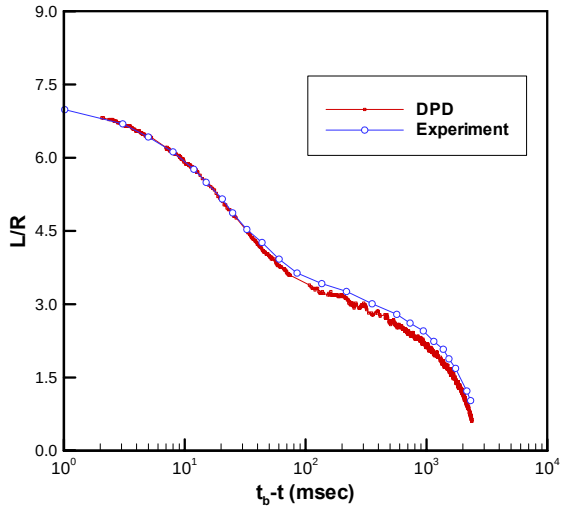


**Figure 9: evolution in time of the dimensionless length of the experimental [5] drop and the DPD drop according to $t_b^{\exp}$**

The smallest distinguished length scale in the DPD simulation is dictated by the volume of a particle $r_p = 0.34 r_c$ which is about $l_T$. Hence, one may conclude that the simulation result below $r_p$ is unacceptable and therefore, the early drop break up can be justified in this way. However, this simulation could also be viewed in a different way. In fact, if the thermal length was used to duplicate the dimensionless numbers, the results of this DPD simulation would be corresponded to the physics of a dripping flow from a nanoscale nozzle with the same thermal length. Accordingly, from this view point, the fast drop break-up, the surface fluctuations and the formation of double-cone structure can be justified. Therefore, it must be noted that the DPD simulations are restricted to the nanoscale problems where the thermal fluctuation effects become important.

## CONCLUSION

In this work, we have used a DPD-based free surface model to simulate the dripping of a mixture of 85% glycerol by weight in water from a nozzle of radius $1600\mu m$. The dripping dynamics is studied as a function of Ohnesorge number, Bond number and Weber number. Therefore, a DPD simulation of dripping is planned to achieve the aforementioned dimensionless numbers without matching the dimensionless thermal length.

The nozzle is constructed with frozen particles and its impenetrability, proper surface wettability, ability to eliminate density oscillation near the wall and no-slip boundary condition is attained by manipulating the coefficient of interacting conservative forces between the wall and the fluid particle. In order to capture the instant geometry of the drop on a Cartesian grid, we assumed that DPD particles should have a volume mass rather than a point mass that carry data through the domain.

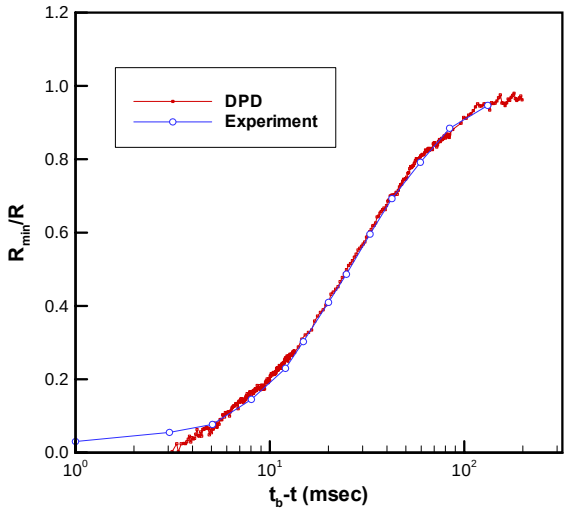


**Figure 10: evolution in time of the dimensionless minimum radius of the experimental [5] thread and the DPD thread according to experiment $t_b^{\exp}$**

Our results are in good agreement with the macroscopic experiment except near the break-up time, when the fluid thread that connects the primitive drop to the nozzle, becomes tenuous. At this point, the DPD simulation comes into question by two issues: the thermal length of the DPD fluid and the finest achievable resolution which is the radius of a particle. The former was much longer than the corresponding value in the experiment. Larger thermal length leads to a break-up which happens before the expected time. However this simulation could be observed in a different way; it can show the physics of a dripping flow from a nanoscale nozzle with the

same thermal length instead. Accordingly in this view the fast drop break-up can be justified.

To conclude, DPD is a powerful method for simulation of free surface flow on different scales but when a phenomenon involves thermal fluctuation, DPD simulation is restricted to nanoscales.

## REFERENCES


[1] Basaran, O. A., 2002, "Small-Scale Free Surface Flows with Breakup: Drop Formation and Emerging Applications," AIChE Journal, 48(9), pp. 1842-1848.

[2] Rothgordt, U., 1978, "Document Printing", Acta Electron, 21(1), pp. 71-82.

[3] Inculet, I. I., 1985, "Industrial Applications of Static Electricity", Journal of Electrostatics, 16(2-3), pp. 287-298.

[4] Wham, R. M., and Byers, C. H., 1985, "Mass Transport from Single Droplets in Imposed Electric Fields", Separation Science and Technology, 22(2-3), pp. 447-466.

[5] Zhang, X., and Basaran, O. A., 1995, "An Experimental Study of Dynamics of Drop Formation", Physics of Fluids, 7(6), pp. 1184-1203.

[6] Schulkes, R. M. S. M., 1994, "Evolution and Bifurcation of a Pendant Drop," Journal of Fluid Mechanics, 278(pp. 83-100.

[7] Eggers, J., 2002, "Dynamics of Liquid Nanojets", Physical Review Letters, 89(8), pp. -.

[8] Kumar, A., Asako, Y., Abu-Nada, E., Krafczyk, M., and Faghri, M., 2009, "From Dissipative Particle Dynamics Scales to Physical Scales: A Coarse-Graining Study for Water Flow in Microchannel", Microfluidics and Nanofluidics, 7(4), pp. 467-477.

[9] Füchslin, R. M., Fellermann, H., Eriksson, A., and Ziock, H. J., 2009, "Coarse Graining and Scaling in Dissipative Particle Dynamics", Journal of Chemical Physics, 130(21), pp.

[10] Clark, A. T., Lal, M., Ruddock, J. N., and Warren, P. B., 2000, "Mesoscopic Simulation of Drops in Gravitational and Shear Fields", Langmuir, 16(15), pp. 6342-6350.

[11] Tiwari, A., and Abraham, J., 2006, "Dissipative-Particle-Dynamics Model for Two-Phase Flows", Phys Rev E Stat Nonlin Soft Matter Phys, 74(5 Pt 2), pp. 056701.

[12] Groot, R., and Warren, P., 1997, "Dissipative Particle Dynamics: Bridging the Gap between Atomistic and Mesoscopic Simulation", The Journal of Chemical Physics, 107(11), pp. 4423-4435.

[13] Espanol, P., and Warren, P., 1995, "Statistical-Mechanics of Dissipative Particle Dynamics", Europhysics Letters, 30(4), pp. 191-196.

[14] Warren, P. B., 2003, "Vapor-Liquid Coexistence in Many-Body Dissipative Particle Dynamics", Physical Review E, 68(6), pp. -.

[15] Pivkin, I. V., and Karniadakis, G. E., 2005, "A New Method to Impose No-Slip Boundary Conditions in Dissipative Particle Dynamics", Journal of Computational Physics, 207(1), pp. 114-128.

[16] Lees, A. W., and Edwards, S. F., 1972, "The Computer Study of Transport Processes under Extreme Conditions", Journal of Physics C: Solid State Physics, 5(15), pp. 1921-1928.

[17] Groot, R. D., and Warren, P. B., 1997, "Dissipative Particle Dynamics: Bridging the Gap between Atomistic and Mesoscopic Simulation", Journal of Chemical Physics, 107(11), pp. 4423-4435.

[18] Eggers, J., 1997, "Nonlinear Dynamics and Breakup of Free-Surface Flows", Reviews of Modern Physics, 69(3), pp. 865-929.

[19] Trofimov, S. Y., Nies, E. L. F., and Michels, M. a. J., 2002, "Thermodynamic Consistency in Dissipative Particle Dynamics Simulations of Strongly Nonideal Liquids and Liquid Mixtures", Journal of Chemical Physics, 117(20), pp. 9383-9394.

[20] Moseler, M. and Landman, U., 2000, "Formation, stability, and breakup of nanojets", *Science*, 289, pp. 1165-1169.